

# Resource Constrained Neural Networks for 5G Direction-of-Arrival Estimation in Micro-controllers

Piyush Sahoo<sup>1</sup>, Romesh Rajoria<sup>1</sup>, Shivam Chandhok<sup>2</sup>, S. J. Darak<sup>1</sup>, Danilo Pau<sup>3</sup>, Hem-Dutt Dabral<sup>4</sup>

<sup>1</sup>Algorithms to Architecture Lab, ECE, IIT Delhi, India

<sup>2</sup>Mohamed bin Zayed University of AI, UAE,

<sup>3</sup>STMicroelectronics, Milan, Italy,

<sup>4</sup>STMicroelectronics, Greater Noida, India.

## ABSTRACT

With the introduction of shared spectrum sensing and beam-forming based multi-antenna transceivers, 5G networks demand spectrum sensing to identify opportunities in time, frequency, and spatial domains. Narrow beam-forming makes it difficult to have spatial sensing (direction-of-arrival, DoA, estimation) in a centralized manner, and with the evolution of paradigms such as artificial intelligence of Things (AIOT), ultra-reliable low latency communication (URLLC) services and distributed networks, intelligence for edge devices (Edge-AI) is highly desirable. It helps to reduce the data-communication overhead compared to cloud-AI-centric networks and is more secure and free from scalability limitations. However, achieving desired functional accuracy is a challenge on edge devices such as microcontroller units (MCU) due to area, memory, and power constraints. In this work, we propose low complexity neural network-based algorithm for accurate DoA estimation and its efficient mapping on the off-the-shelf MCUs. An ad-hoc graphical-user interface (GUI) is developed to configure the STM32 NUCLEO-H743ZI2 MCU with the proposed algorithm and to validate its functionality. The performance of the proposed algorithm is analyzed for different signal-to-noise ratios (SNR), word-length, the number of antennas, and DoA resolution. In-depth experimental results show that it outperforms the conventional statistical spatial sensing approach.

## KEYWORDS

DoA estimation, edge-AI, 5G, neural networks, X-CUBE-AI, micro-controller, STM32

### ACM Reference Format:

Piyush Sahoo<sup>1</sup>, Romesh Rajoria<sup>1</sup>, Shivam Chandhok<sup>2</sup>, S. J. Darak<sup>1</sup>, Danilo Pau<sup>3</sup>, Hem-Dutt Dabral<sup>4</sup>, <sup>1</sup>Algorithms to Architecture Lab, ECE, IIT Delhi, India, <sup>2</sup>Mohamed bin Zayed University of AI, UAE, <sup>3</sup>STMicroelectronics, Milan, Italy, <sup>4</sup>STMicroelectronics, Greater Noida, India, . 2021. Resource Constrained Neural Networks for 5G Direction-of-Arrival Estimation in Micro-controllers. In *Proceedings of First International Conference on AI-ML Systems (AIMLSystems '21)*. ACM, New York, NY, USA, 7 pages. <https://doi.org/10.1145/nnnnnnnn.nnnnnnnn>

Permission to make digital or hard copies of all or part of this work for personal or classroom use is granted without fee provided that copies are not made or distributed for profit or commercial advantage and that copies bear this notice and the full citation on the first page. Copyrights for components of this work owned by others than ACM must be honored. Abstracting with credit is permitted. To copy otherwise, or republish, to post on servers or to redistribute to lists, requires prior specific permission and/or a fee. Request permissions from [permissions@acm.org](mailto:permissions@acm.org).

*AIMLSystems '21, Oct. 21–23, 2021, Bangalore, India*

© 2021 Association for Computing Machinery.

ACM ISBN 978-x-xxxx-xxxx-x/YY/MM. . \$15.00

<https://doi.org/10.1145/nnnnnnnn.nnnnnnnn>

## 1 INTRODUCTION

A never-ending expansion of network connectivity has led to the evolution of the Internet of things (IoT) capable to route heterogeneous information between people and devices on a planetary scale [8, 9, 37]. From simple temperature and pressure sensors to smart home and smart industry processing units relying on faster networks, IoT has resulted in exponential growth, offering increased productivity, better security, as well as the availability of a huge amount of business-worth data [8, 9, 37]. The analysis of such data to get useful trends and patterns is itself a challenging task and recent progress in Artificial Intelligence (AI) has led to promising solutions for exploiting the hidden information and correlations embodied into the data [4, 23, 46]. Conventional cloud-AI IoT networks perform data processing and inferences at resource-rich data centers. Unfortunately, such a centralized approach suffers from data-communication overhead, high unpredictable latency, low security, privacy, and poor scalability [6, 22, 25, 39]. Furthermore, data centers are not environmentally friendly, energy parsimonious, and green [13].

To overcome some of these challenges, the Edge-AI distributed approach is being considered as a solution in which edge devices are featuring intelligence to perform inference either independently or in collaboration with other processing units [6, 22, 25, 39]. Edge-AI is being actively explored for speech, video, environmental, industry 4.0, and autonomous driving applications. For instance, edge-AI includes assisting devices such as cognitive hearing aids [40], optical character recognition [5, 28], and smart home appliances such as google home, Alexa, etc. With the introduction of shared spectrum sensing due to limited spectrum availability, 5G networks demand spectrum sensing to identify spectrum opportunities in time, frequency and spatial domains [3, 24, 35]. The beam-forming based multi-antenna transceivers allow spatially separated users to communicate simultaneously over the common spectrum leading to significant improvement in network throughput [14]. However, narrow beam-forming makes it difficult to have spatial sensing (direction-of-arrival, DoA, estimation) in a centralized manner, and hence, intelligence at user devices is highly desirable. Edge-AI is also important to bring next-generation computing paradigms such as artificial intelligence of Things (AIOT), ultra-reliable low latency communication (URLLC) services, smart industry 4.0, and distributed networks to reality [12, 42].

In the last decade, machine and deep learning algorithms have significantly outperformed hand-crafted rule-based and classic machine learning approaches in various application domains. In wireless communications, deep learning algorithms are widely used for

spectrum sensing and characterization, channel estimation, and resource allocations [27, 41, 43]. However, most of their deployment is limited to cloud-AI networks due to the availability of virtually unlimited resources (memory, computational power, etc.). The deployment of these algorithms in Edge-AI networks needs careful design and low power mapping on hardware since achieving the desired target accuracy is a challenge due to area, memory and power-constrained micro-controller units (MCU) usually feature. The work presented in this paper attempts to address these challenges for spatial sensing applications in wireless networks by targeting the highest accuracy with the lowest implementation costs and using the MCU resources parsimoniously.

### 1.1 Problem Formulation

The goal of this work is to develop a lightweight DoA estimation framework using artificial neural networks that can be easily deployed on off-the-shelf resource-constrained MCUs. Various works have explored DoA estimation for wireless signals and its implementation on hardware such as FPGA/ASICs [18, 19, 26]. To the best of our knowledge, DoA estimation for wireless signals using neural networks for MCUs has not been explored yet in the literature and is the focus of the proposed work. The DoA estimation-based spatial sensing is also useful in radar, sonar, and navigation to track an object, biomedical to detect tumors, and artery wall movements.

We consider the analog-front-end with multiple antennas and assume that the MCU receives a baseband signal consisting of one active transmission with unknown DoA. The problem of DOA estimation can be formulated as a  $K$  class classification problem, where each class corresponds to a possible angle or direction of signal arrival, depending on the antenna-array placement and desired resolution. Given an angle range  $A$  of antenna array and a specific DoA resolution  $R$ , we define a set of DoA classes  $C = \{c_1, c_2, c_3, \dots, c_K\}$ , where the number of classes,  $K = A/R$ . In most of the cases,  $A = 360^\circ$ . Figure 1 shows the overall architecture of the proposed DoA estimation framework using a deep-learning-based supervised learning paradigm. Formally, we first generate the training and testing data following the wideband signal generation model described in Section 2.1. We then devise a lightweight neural network architecture and train a deep learning-based DoA classification model as described in Section 2.2. Finally, we develop a GUI interface for deployment and performance validation as discussed in Section 3. Experimental results are discussed in Section 4 and Section 5 concludes the paper.

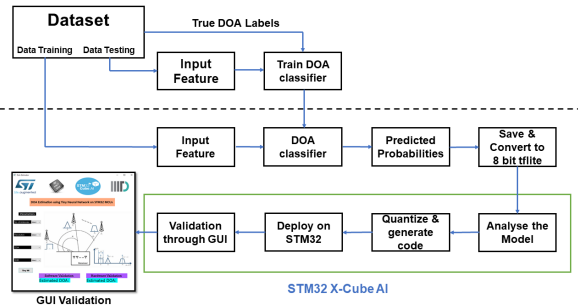


Figure 1: Overall architecture for the proposed DoA estimation framework.

## 2 PROPOSED WORK

In this section, we discuss the wireless signal model used to generate the dataset and, the design details of the neural network used to estimate the DoA.

### 2.1 Wireless Signal Model for Dataset

We consider a wideband spectrum consisting of several disjoint, uncorrelated, and far-field signals. These signals are imposed on the  $L$ -antenna receiver with either Uniform Linear Array (ULA). The signal received at the  $l^{\text{th}}$  antenna is defined as follows:

$$x_l(t) = \sum_{m=1}^M a_m(t - \tau_l(\theta_m)) e^{j2\pi f_m(t - \tau_l(\theta_m))} + n_l(t) \quad (1)$$

$$\approx \sum_{m=1}^M a_m(t) e^{j2\pi f_m(t - \tau_l(\theta_m))} + n_l(t) \quad (2)$$

where  $M$  is the number of narrow band signals,  $a_m(t)$  is the amplitude of  $m^{\text{th}}$  narrowband signal of carrier frequency,  $f_m$  and DoA,  $\theta_m$ . Furthermore,  $\tau_l(\theta_m)$  is the time delay observed by the  $m^{\text{th}}$  signal at the  $l^{\text{th}}$  antenna and  $n_l(t)$  is the additive white Gaussian noise (AWGN) at the  $l^{\text{th}}$  antenna based on the SNR of the communication channel. The output of the  $l^{\text{th}}$  antenna is digitized by means of Nyquist sampling where the received signal,  $x_l(t)$  is mixed with a mixing function,  $m(t) = \sum_{b \in \beta} \alpha_{l,b} e^{-j2\pi(b-1)Bt}$  as shown in Fig. 2. Digitization is performed on the set of non-contiguous frequency bands i.e.  $\beta \in \{1, 2, \dots, N\}$ . Here,  $N$  is the total number of non-overlapping frequency bands in the wideband spectrum,  $\alpha_{l,b}$  is a mixing coefficient of  $b^{\text{th}}$  frequency band at  $l^{\text{th}}$  antenna carefully chosen from the Gaussian distribution, and  $B$  is the bandwidth of a frequency band. Next we define the Fourier transform (FT) of the mixed signal,  $\tilde{x}_l(t)$ , as follows

$$\tilde{X}_l(f) = \sum_{m=1}^M e^{j2\pi f_m \tau_l(\theta_m)} \sum_{b \in \beta} \alpha_{l,b} A_m(f - (f_m - (b-1)B)) \quad (3)$$

where  $A_m(f)$  is the FT of  $m^{\text{th}}$  signal. The mixed signal is passed through the low pass filter (LPF) of cut-off frequency  $B/2$  as  $\tilde{X}_l(f)$  covers images over the entire frequency. From the LPF, we get the filtered signal which is digitized at a rate of  $B$  Hz. The output of the ADC can be expressed as

$$Y_l(e^{j2\pi fNT}) = \sum_{b \in \beta_{\text{busy}}} \alpha_{l,b} A_b(f - (f_b - (b-1)B)) e^{j2\pi f_b \tau_l(\theta_b)} \quad (4)$$

where  $\beta_{\text{busy}} \in \beta$  is a selected set of occupied frequency bands,  $A_b(f)$  is the FT of the signal in  $b^{\text{th}}$  frequency band with frequency and DoA of  $f_b$  Hz and  $\theta_b$ , respectively. The FT of the output of all

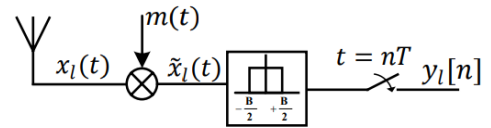


Figure 2: Wideband spectrum digitization approach for dataset generation.

$L$  antennas in the matrix form is given as

$$\mathbf{Y}(f) = \mathbf{S} \mathbf{Z}(f) \quad (5)$$

where  $\mathbf{S}$  is a  $L \times M$  steering matrix where  $\mathbf{S}_{l,m} = e^{j2\pi f_m \tau l(\theta_m)}$ . Note that the steering matrix,  $\mathbf{S}$  contains two variables, carrier frequency,  $f_m$  and DoA,  $\theta_m$  for each of the narrowband signal. The signal received at the antennas is added with AWGN noise based on the SNR value of the channel to generate the final signal corresponding to the combination of DoA and SNR values. In this work, we focus on DoA estimation with known carrier frequency and hence, one frequency band is passed to neural network at a time. The details of dataset generation are given in Section 4.

## 2.2 Neural Network Architecture

In this section, the proposed neural network architecture for DoA estimation is presented. Specifically, we use a convolution-based neural network (CNN) due to their capability in capturing spatial correlations within input signals at different scales (or receptive field) as demonstrated in various computer vision [16, 17, 21, 32–34, 36] and signal processing [7, 29, 30, 44] applications. They are also data-efficient due to the inherent inductive bias of convolution operations [11]. Furthermore, CNNs use parameter sharing across inputs, employ operations that are easily both parallelizable and pipelined and entail  $O(1)$  sequential operations. This is in contrast to recurrent networks (RNN) which employ sequential processing leading to higher inference time or fully connected networks (FCN), which require more parameters and thus more computational efforts and storage resources when compared with the CNN counterparts [31, 45]. Furthermore, CNNs are designed to seamlessly work with spatial signals which are in contrast to FCN or RNNs which require additional processing steps to tackle spatial input data. Thus, we choose CNN for building a lightweight memory efficient, therefore deployable on MCU, framework.

The proposed CNN model consists of a total of 7 layers. The first two layers are 2D convolutional layers with kernel size  $2 \times 2$  and Rectified Linear Unit (ReLU) [2] activation function. Over multiple experiments, we observed that using ReLU allows faster convergence, to learn and perform better. The proposed architecture also includes two 2D max-pooling layers in between which enable progressive reduction of the activations spatial size, reduce the parameters and computational complexity of the network. Finally, we have two Fully Connected Layers (FC). The first FC layer uses ReLU and the last layer has a softmax function which maps the outputs to probability values for classification. We train our model end-to-end with categorical cross-entropy loss. For training it, we use the Adam optimizer [20] due to its training stability and fast convergence properties. Specifically, we use a learning rate of 0.0001 and  $\beta_1 = 0.5$ ,  $\beta_2 = 0.999$  parameters for Adam the optimizer. Our network is implemented using Keras library [10] with Tensorflow backend [1]. Due to limited space constraints, we have not reported various CNN configurations explored during this project. The discussion is limited to a model which offered the best performance fitting also memory constraints of the MCU.

The next step is to pre-process the model for deployment on the chosen micro-controller and corresponding steps are given in Fig.

3. Depending on the application requirements, the model is quantized with appropriate word length (WL). Currently, three WLs, 64-bit double-precision floating-point (DPFL), 32-bit single-precision floating-point (SPFL), and 8-bit integer (INT8) are supported. The quantized model is then exported to as a frozen .pb graph and the file footprint is reduced by discarding metadata and gradient information that were needed during the training procedure. The frozen graph is then converted to the tflite file using the Tensorflow lite conversion procedure. The resulting file is then used to deploy it on the STM32 MCU taking advantage of the X-CUBE-AI automatic deployment procedure integrated into STM32CubeMX [38]. Please refer to video tutorials ([demo link](#)) explaining the detailing function of the proposed DoA estimation framework.

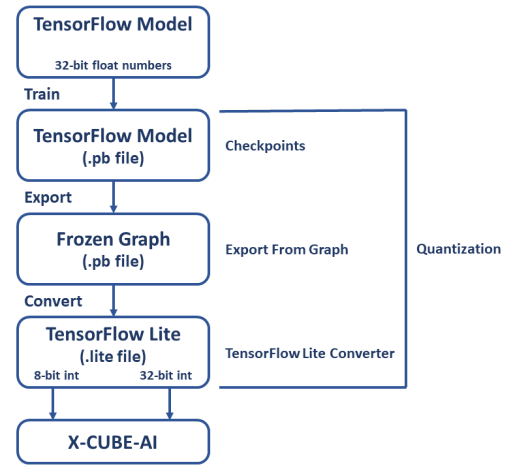
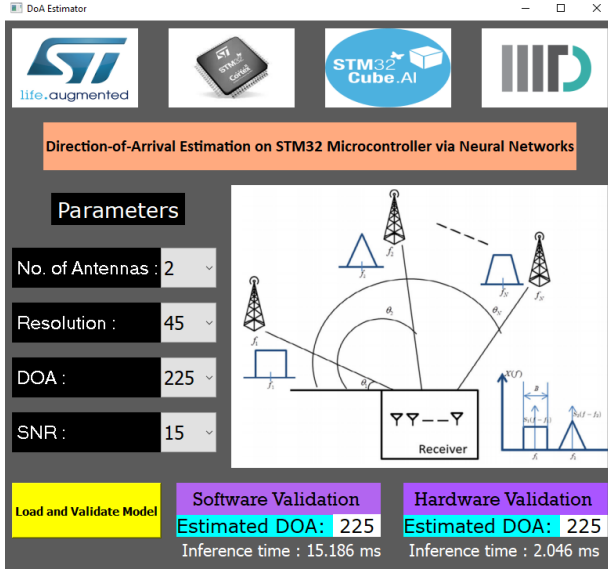


Figure 3: Block diagram depicting the tensorflow steps used to convert proposed CNN model in tflite format that can be deployed on the STM32 micro-controller.

## 3 GUI FOR MODEL DEPLOYMENT ON MCU

The deployment of the neural network model on a micro-controller and its performance analysis needs an appropriate user-friendly Graphical User Interface (GUI). Such GUI is application-dependent and needs to be developed from scratch. In this section, we provide details of the proposed GUI which enabled validation of the CNN model on the NUCLEO-H743ZI2 board and comparison with x86 software implementation. Fig. 4 shows the proposed GUI in which users can configure the system parameters such as SNR, number of antennas ( $L$ ), DoA resolution ( $R$ ), and DoA of the active signal along with an appropriate model for a given word-length (WL). The GUI then generates appropriate test data, validates the desired model on the Nucleo-STM32 board, and displays the results given by the software (x86) and hardware (STM32) implementations along with the inference time.

To perform the validation on Nucleo-STM32H743ZI2, we develop seamless interaction between the GUI interface and Nucleo-STM32 board to communicate model files and input/output data. In this work, we used X-CUBE-AI-based python libraries to establish the communication between the PC and the NUCLEO-STM32 MCU. There are two python modules composing the HOST API package



**Figure 4: Proposed GUI to validate the neural-network models in both x86 software and NUCLEO-STM32 hardware modes.**

which play an important role in validating generated neural networks running on a Nucleo-STM32 board connected to the host PC using a standard serial interface (ST-Link V2/V3 virtual com port).

The first module is *stm32nn* which allows discovering the neural networks which are available in the Nucleo-STM32 firmware. It enables GUI application to retrieve important characteristics of the deployed neural network (tensor input/output format, multiply-accumulate operation complexity, RAM/ROM size used by CNN, etc.) and perform inference with the client data (default mode). Furthermore, it also helps to establish the UART communication with the Nucleo-STM32 board. The second module is the *stm32pb* which implements the low-level input/output functions required to communicate with the firmware running on the STM32 device. This firmware communicates with the GUI through the UART interface. For doing Nucleo-STM32 validation we deployed the X-CUBE-AI automatically generated aiValidaiton-application on the edge device (Nucleo-STM32 board) with the help of STM32CubeIDE which is an Integrated Development Environment for STM32 Microcontrollers. This is a built-in application of X-CUBE-AI that doesn't require any handcrafting to be deployed on Nucleo-STM32.

We used the Nucleo-STM32H743ZI2 board to validate our DoA estimation application. This board features a STM32H743ZI2 MCU (ARM Cortex-M7 core based) which allows IoT practitioners to choose among different combinations of performance and power consumption by selecting among four different CPU run-modes namely Range-0 to Range-3. Run mode Range-0 provides the highest performance at the cost of higher power consumption. Successive run-modes (Range-1, Range-2, and Range-3) can be used to lower the system's power consumption and performance by lowering the CPU operating frequency. STM32H743ZI2 MCU can run at clock frequencies of up to 480MHz and embeds 1 MByte RAM and 2 MBytes of non-volatile flash memory. Due to memory constraints,

we need to optimize the size of the CNN model which can be embedded into it. X-CUBE-AI expansion (of STM32CubeMX) package was used to automatically generate STM32-optimized C-code and run time library corresponding to application-specific, pre-trained CNN model. Using X-CUBE-AI, multiple neural network models can be embedded into the STM32H743ZI2 microcontroller provided that the combined size of all the models is within the memory limit of the STM32H743ZI2. The GUI application also validates the performance of the model on the host processor (x86), which is another feature of X-CUBE-AI. It uses the TensorFlow Lite model file (.tflite) to validate the accuracy of the neural network library generated by X-CUBE-AI. For GUI design, the PyQt5 python library and Qt Designer platform is used for adding different features to make GUI user-friendly.

## 4 EXPERIMENTS AND PERFORMANCE ANALYSES

In this section, we describe the experimental setup and characterize the performances of the proposed framework in comparison with baseline approaches for different values of  $R$ ,  $L$ , SNR, and WL. We begin with the details of the dataset generated in this project.

**Proposed Dataset:** The proposed dataset is generated by using the wideband signal model (described in section 2.1) and MATLAB software. The data generation code requires various input parameters such as  $R$ , SNR,  $L$ , sampling frequency, and the number of observations  $N$ . For the experiments presented in this section, we consider five different DoA resolutions, 5 different size antenna arrays, and 20 different SNR values as shown in Table 1. Thus, the total number of DoA classes ranges from 8 in  $R = 45$  to 40 in  $R = 9$ . We generate  $N = 2500$  observations for each DoA class. Each observation or data point comprises of complex-valued signal of dimension  $l \times d$ , where  $d$  denotes the dimension of each signal and  $l$  is the *antenna count*. The complex-valued data is then converted into the real and imaginary parts. Unfortunately to date, Since Keras does not handle natively complex numbers, they are then concatenated with each other to form a combined matrix of size  $(l * 2) \times d$ , which acts as the input to the neural network. We keep 80% samples as a training set and 20% for the test set. Furthermore, out of the training set, 20% samples are kept aside as a validation set. All datasets are free and available online ([here](#)).

Antenna Count ( $L$ )	2-6
DoA Resolution ( $R$ )	45, 36, 24, 18, 9
SNR	0-20dB
DoA classes	$K = 360/R$
Observations ( $N$ )	2500 per class

**Table 1: Summary of signal parameters used for dataset generation**

First, we begin with analyzing the effect of  $L$  on the DoA estimation accuracy for different SNRs and  $R$ . In Fig. 5, we compare the DoA accuracy for dataset with fixed DoA resolution of 45. Here, we vary the number of antennas from 2-6 and the SNR range is 0-20 dB. It can be observed that the DoA accuracy increases significantly



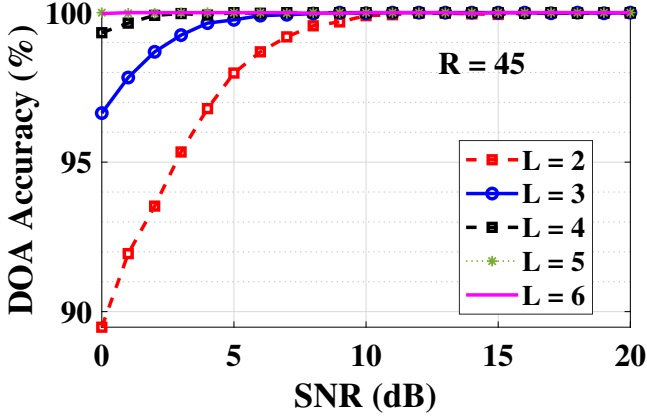


Figure 5: Comparison of DoA accuracy in % for different values of  $L$  and SNRs with a fixed  $R = 45$ .

with the increase in the number of antennas due to additional information gained via a signal received from the spatially separated antenna elements. Furthermore, DoA accuracy increases with the increase in SNR due to the reduced impact of noise. Note that the increase in DoA estimation accuracy with the increase in the number of antennas is substantial at low SNR. Furthermore, for the model with only 2 antennas, the average validation accuracy is 96% and the average test accuracy is 95.6% over the chosen SNR range. In Fig. 6, we repeat the same experiments for the dataset with the DoA resolution of 36 i.e. more number of candidate DoAs. The results are similar to Fig. 5 except for slight degradation in estimation accuracy. From Fig. 5 and Fig. 6, we can conclude that the higher the number of antennas, higher is the accuracy. However, the gain in performance is not significant for the higher number of antennas which means the number of antennas must be selected carefully. This is because an increase in the number of antennas results in an increase in the area and power complexity of the analog front-end due to multiple radio-frequency chains and higher computational complexity of digital-front-end and baseband algorithms due to a higher number of digitized samples.

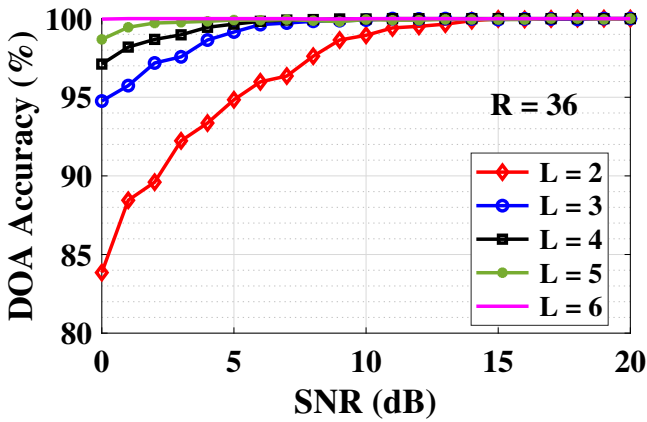


Figure 6: Comparison of DoA accuracy in % for different values of  $L$  and SNRs with a fixed  $R = 36$ .

Next, we study the difference in the DoA estimation accuracy for different  $R$  and subsequent improvement after increasing  $L$ . In Fig. 7, it can be observed that the DoA estimation accuracy decreases significantly with the decrease in the DoA resolution. This is due to the increase in the number of classes with the decrease in  $R$  making a classification problem more challenging. To further increase the accuracy, we need to increase the number of antennas, especially at low SNRs. This also demands a reconfigurable antenna and DoA estimation architecture that can adapt based on the desired accuracy. Similarly, we study the difference in the DoA estimation accuracy for different  $R$  and subsequent improvement after increasing SNR. Since SNR depends on the wireless environment, it can not be controlled and hence, the wireless channel, with the desired SNR, must be chosen via appropriate resource allocation strategies.

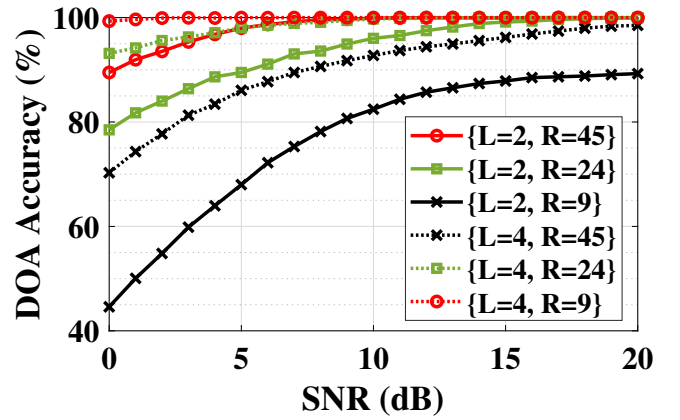


Figure 7: Comparison of the effect of  $R$  and  $L$  on the DoA accuracy in % for different SNR.

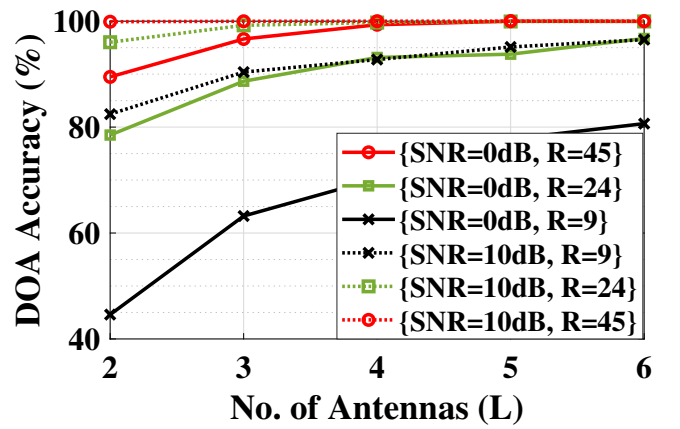
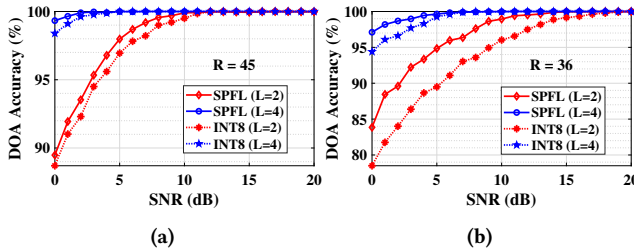


Figure 8: Comparison of the effect of  $R$  and SNR on the DoA accuracy in % for different  $L$ .

Next, we study the effect of word length on the performance of the proposed algorithm. As shown in Fig. 9a and Fig. 9b, WL of 8-bit integer results in slight degradation of the performance compared to SPFL WL. We also observed that the SPFL and DPFL WLs offer nearly identical performance and the DPFL results are

excluded to maintain the clarity of the plots. The WL optimization is critical to meet the memory constraints of the micro-controller. For instance, the proposed algorithm with  $R = 45$ , and  $L = 2$  needs 0.8 Mebibyte (MiB) and 0.3 kibibytes (KiB) flash and on-chip RAM, respectively for SPFL WL. This reduces to 0.2 MiB (-25%) and 0.09 KiB (-33%) of flash and on-chip RAM, respectively for INT8 WL. Furthermore, the number of multiply-accumulate computations is reduced from 431560 SPFL operations to 424568 INT8 operations. This has resulted in the reduction in execution time from 6.4 ms to 2 ms (-32%). Thus, careful selection of WL can offer significant savings in memory, computational complexity and execution time without compromising on the DoA estimation accuracy significantly.



**Figure 9: Comparison of the effect of WL on the DoA accuracy in % for (a)  $R = 45$  and (b)  $R = 36$  with  $L = \{2, 4\}$ .**

In the end, we present the comparison of the proposed algorithm with the well-known spatial spectrum estimation approach known as the Multiple Signal Classification (MUSIC) algorithm [15]. The basic idea of the MUSIC algorithm is to perform characteristic decomposition of the covariance matrix of an array output data, resulting in a signal subspace orthogonal with a noise subspace corresponding to the signal components. The two orthogonal subspaces are then used to constitute a spectrum function that can be used for spectral peak search and detect DoA signals [15]. In Fig. 10a, we compare the performance of proposed and MUSIC algorithms for  $R = \{45, 36\}$  with  $L = 2$ . It can be observed that the proposed algorithm outperforms MUSIC at all SNRs and offers an average of 5% higher accuracy. As shown in Fig. 10b, the performance of both algorithms improves with the increase in  $L$  from 2 to 4. However, the gain in performance is significant in the proposed algorithm compared to MUSIC due to carefully designed CNN architecture exploiting the spatial information received from additional antennas.

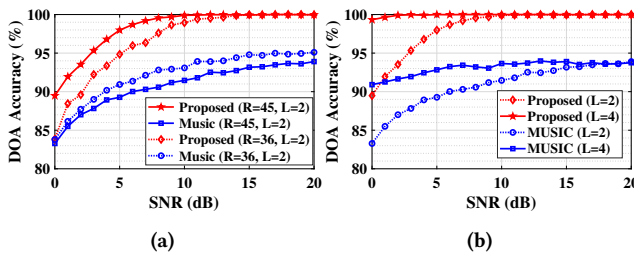


**Figure 10: Comparison of DoA accuracy in % for MUSIC and proposed approach for: (a) Different  $R$ , and (b) Different  $L$ .**

## 5 CONCLUSION

In this work, we developed a lightweight, accurate deep learning-based framework for the task of direction-of-arrival (DoA) estimation in wireless networks. We developed a user-friendly graphical user interface (GUI) to deploy and validate the performance of the proposed algorithm on any micro-controller such as the STM32H743ZI2 development board. In-depth performance analysis for different signal-to-noise ratios (SNR), word-length, number of antennas, and DoA resolution validated the superiority of the proposed algorithm over the state-of-the-art approach. Future works include the extension of the proposed framework for multi-band DoA classification and real-time tracking of DoA for upcoming vehicular networks. Furthermore, we would like to incorporate the support for additional word lengths such as INT16 and INT32 which are not available in existing tools.

## REFERENCES

- [1] Martín Abadi, Ashish Agarwal, Paul Barham, Eugene Brevdo, Zhifeng Chen, Craig Citro, Greg S. Corrado, Andy Davis, Jeffrey Dean, Matthieu Devin, Sanjay Ghemawat, Ian Goodfellow, Andrew Harp, Geoffrey Irving, Michael Isard, Yangqing Jia, Rafal Jozefowicz, Lukasz Kaiser, Manjunath Kudlur, Josh Levenberg, Dandelion Mané, Rajat Monga, Sherry Moore, Derek Murray, Chris Olah, Mike Schuster, Jonathon Shlens, Benoit Steiner, Ilya Sutskever, Kunal Talwar, Paul Tucker, Vincent Vanhoucke, Vijay Vasudevan, Fernanda Viégas, Oriol Vinyals, Pete Warden, Martin Wattenberg, Martin Wicke, Yuan Yu, and Xiaoqiang Zheng. 2015. TensorFlow: Large-Scale Machine Learning on Heterogeneous Systems. <https://www.tensorflow.org/> Software available from tensorflow.org.
- [2] Abien Fred Agarap. 2018. Deep Learning using Rectified Linear Units (ReLU). *ArXiv abs/1803.08375* (2018).
- [3] W. S. H. M. W. Ahmad, N. A. M. Radzi, F. S. Samidi, A. Ismail, F. Abdullah, M. Z. Jamaludin, and M. N. Zakaria. 2020. 5G Technology: Towards Dynamic Spectrum Sharing Using Cognitive Radio Networks. *IEEE Access* 8 (2020), 14460–14488. <https://doi.org/10.1109/ACCESS.2020.2966271>
- [4] Mohammed Ali Al-Garadi, Amr Mohamed, Abdulla Khalid Al-Ali, Xiaojiang Du, Ihsan Ali, and Mohsen Guizani. 2020. A Survey of Machine and Deep Learning Methods for Internet of Things (IoT) Security. *IEEE Communications Surveys Tutorials* 22, 3 (2020), 1646–1685. <https://doi.org/10.1109/COMST.2020.2988293>
- [5] Syed Umar Amin and M. Shamim Hossain. 2021. Edge Intelligence and Internet of Things in Healthcare: A Survey. *IEEE Access* 9 (2021), 45–59. <https://doi.org/10.1109/ACCESS.2020.3045115>
- [6] Stephen Cass. 2019. Taking AI to the edge: Google’s TPU now comes in a maker-friendly package. *IEEE Spectrum* 56, 5 (2019), 16–17. <https://doi.org/10.1109/MSPEC.2019.8701189>
- [7] Shivam Chandhok, H. Joshi, A. Subramanyam, and S. Darak. 2019. Novel Deep Learning Framework for Wideband Spectrum Characterization at Sub-Nyquist Rate. *arXiv: Signal Processing* (2019).
- [8] Zhuoqing Chang, Shubo Liu, Xingxing Xiong, Zhaohui Cai, and Guoqing Tu. 2021. A Survey of Recent Advances in Edge-Computing-Powered Artificial Intelligence of Things. *IEEE Internet of Things Journal* (2021), 1–1. <https://doi.org/10.1109/JIOT.2021.3088875>
- [9] Lalit Chettri and Rabindranath Bera. 2020. A Comprehensive Survey on Internet of Things (IoT) Toward 5G Wireless Systems. *IEEE Internet of Things Journal* 7, 1 (2020), 16–32. <https://doi.org/10.1109/JIOT.2019.2948888>
- [10] François Chollet et al. 2015. Keras. <https://keras.io>.
- [11] Nadav Cohen and A. Shashua. 2017. Inductive Bias of Deep Convolutional Networks through Pooling Geometry. *ArXiv abs/1605.06743* (2017).
- [12] Mischa Dohler, Toktam Mahmoodi, Maria A. Lema, Massimo Condoluci, Fragkiskos Sardinis, Konstantinos Antonakoglou, and Hamid Aghvami. 2017. Internet of skills, where robotics meets AI, 5G and the Tactile Internet. In *2017 European Conference on Networks and Communications (EuCNC)*. 1–5. <https://doi.org/10.1109/EuCNC.2017.7980645>
- [13] Joao Ferreira, Gustavo Callou, Albert Josua, and Paulo Maciel. 2018. Estimating the Environmental Impact of Data Centers. In *2018 IEEE 17th International Symposium on Network Computing and Applications (NCA)*. 1–4. <https://doi.org/10.1109/NCA.2018.8548326>
- [14] Zhen Gao, Linglong Dai, Wei Dai, Byonghyo Shim, and Zhaocheng Wang. 2016. Structured Compressive Sensing-Based Spatio-Temporal Joint Channel Estimation for FDD Massive MIMO. *IEEE Transactions on Communications* 64, 2 (2016), 601–617. <https://doi.org/10.1109/TCOMM.2015.2508809>
- [15] Pooja Gupta and S.P. Kar. 2015. MUSIC and improved MUSIC algorithm to estimate direction of arrival. In *2015 International Conference on Communications*

- and *Signal Processing (ICCSPP)*, 0757–0761. <https://doi.org/10.1109/ICCSPP.2015.7322593>
- [16] Kaiming He, Georgia Gkioxari, Piotr Dollár, and Ross B. Girshick. 2017. Mask R-CNN. *2017 IEEE International Conference on Computer Vision (ICCV)* (2017), 2980–2988.
- [17] Kaiming He, X. Zhang, Shaoqing Ren, and Jian Sun. 2016. Deep Residual Learning for Image Recognition. *2016 IEEE Conference on Computer Vision and Pattern Recognition (CVPR)* (2016), 770–778.
- [18] Ahmed A. Hussain, Nizar Tayem, Muhammad Omair Butt, Abdel-Hamid Soliman, Abdulrahman Alhamed, and Saleh Alshebeili. 2018. FPGA Hardware Implementation of DOA Estimation Algorithm Employing LU Decomposition. *IEEE Access* 6 (2018), 17666–17680. <https://doi.org/10.1109/ACCESS.2018.2820122>
- [19] Himani Joshi, Sumit J. Darak, Mohammad Alae-Kerahroodi, and Bhavani Shankar Mysore Rama Rao. 2021. Reconfigurable and Intelligent Ultra-wideband Angular Sensing: Prototype Design and Validation. *IEEE Transactions on Instrumentation and Measurement* 70 (2021), 1–15. <https://doi.org/10.1109/TIM.2021.3058406>
- [20] Diederik P. Kingma and Jimmy Ba. 2015. Adam: A Method for Stochastic Optimization. *CoRR* abs/1412.6980 (2015).
- [21] A. Krizhevsky, Ilya Sutskever, and Geoffrey E. Hinton. 2012. ImageNet classification with deep convolutional neural networks. *Commun. ACM* 60 (2012), 84–90.
- [22] En Li, Liekang Zeng, Zhi Zhou, and Xu Chen. 2020. Edge AI: On-Demand Accelerating Deep Neural Network Inference via Edge Computing. *IEEE Transactions on Wireless Communications* 19, 1 (2020), 447–457. <https://doi.org/10.1109/TWC.2019.2946140>
- [23] He Li, Kaoru Ota, and Mianxiong Dong. 2018. Learning IoT in Edge: Deep Learning for the Internet of Things with Edge Computing. *IEEE Network* 32, 1 (2018), 96–101. <https://doi.org/10.1109/MNET.2018.1700202>
- [24] S. Y. Lien, S. L. Shieh, Y. Huang, B. Su, Y. L. Hsu, and H. Y. Wei. June 2017. 5G New Radio: Waveform, Frame Structure, Multiple Access, and Initial Access. *IEEE Communication Magazine* 55 (June 2017), 64–71.
- [25] Sen Lin, Zhi Zhou, Zhaofeng Zhang, Xu Chen, and Junshan Zhang. 2020. Edge Intelligence in the Making: Optimization, Deep Learning, and Applications.
- [26] Zhang-Meng Liu, Chenwei Zhang, and Philip S. Yu. 2018. Direction-of-Arrival Estimation Based on Deep Neural Networks With Robustness to Array Imperfections. *IEEE Transactions on Antennas and Propagation* 66, 12 (2018), 7315–7327. <https://doi.org/10.1109/TAP.2018.2874430>
- [27] Qian Mao, Fei Hu, and Qi Hao. 2018. Deep Learning for Intelligent Wireless Networks: A Comprehensive Survey. *IEEE Communications Surveys Tutorials* 20, 4 (2018), 2595–2621. <https://doi.org/10.1109/COMST.2018.2846401>
- [28] Jamshed Memon, Maira Sami, Rizwan Ahmed Khan, and Mueen Uddin. 2020. Handwritten Optical Character Recognition (OCR): A Comprehensive Systematic Literature Review (SLR). *IEEE Access* 8 (2020), 142642–142668. <https://doi.org/10.1109/ACCESS.2020.3012542>
- [29] T. O’Shea, Johnathan Corgan, and T. Clancy. 2016. Convolutional Radio Modulation Recognition Networks. *ArXiv abs/1602.04105* (2016).
- [30] T. O’Shea, Tamoghna Roy, and T. Clancy. 2018. Over-the-Air Deep Learning Based Radio Signal Classification. *IEEE Journal of Selected Topics in Signal Processing* 12 (2018), 168–179.
- [31] Sudeep Raja. 2021. FNNs, RNNs, LSTM and BLSTM. <http://cse.iitkgp.ac.in/~psraja/FNNs%20RNNs%20LSTM%20and%20BLSTM.pdf>
- [32] Joseph Redmon, S. Divvala, Ross B. Girshick, and A. Farhadi. 2016. You Only Look Once: Unified, Real-Time Object Detection. *2016 IEEE Conference on Computer Vision and Pattern Recognition (CVPR)* (2016), 779–788.
- [33] Shaoqing Ren, Kaiming He, Ross B. Girshick, and J. Sun. 2015. Faster R-CNN: Towards Real-Time Object Detection with Region Proposal Networks. *IEEE Transactions on Pattern Analysis and Machine Intelligence* 39 (2015), 1137–1149.
- [34] O. Ronneberger, P. Fischer, and T. Brox. 2015. U-Net: Convolutional Networks for Biomedical Image Segmentation. In *MICCAI*.
- [35] Shree Krishna Sharma, Tadilo Endeshaw Bogale, Long Bao Le, Symeon Chatzinoas, Xianbin Wang, and Björn Ottersten. 2018. Dynamic Spectrum Sharing in 5G Wireless Networks With Full-Duplex Technology: Recent Advances and Research Challenges. *IEEE Communications Surveys Tutorials* 20, 1 (2018), 674–707. <https://doi.org/10.1109/COMST.2017.2773628>
- [36] Evan Shelhamer, Jonathan Long, and Trevor Darrell. 2017. Fully Convolutional Networks for Semantic Segmentation. *IEEE Transactions on Pattern Analysis and Machine Intelligence* 39 (2017), 640–651.
- [37] Weisong Shi, Jie Cao, Quan Zhang, Youhuizi Li, and Lanyu Xu. 2016. Edge Computing: Vision and Challenges. *IEEE Internet of Things Journal* 3, 5 (2016), 637–646. <https://doi.org/10.1109/JIOT.2016.2579198>
- [38] STMicroelectronics. [n.d.]. STM32CubeMX. <https://www.st.com/en/development-tools/stm32cubemx.html>
- [39] Marian Verhelst and Bert Moons. 2017. Embedded Deep Neural Network Processing: Algorithmic and Processor Techniques Bring Deep Learning to IoT and Edge Devices. *IEEE Solid-State Circuits Magazine* 9, 4 (2017), 55–65. <https://doi.org/10.1109/MSSC.2017.2745818>
- [40] DeLiang Wang. 2017. Deep Learning Reinvents the Hearing Aid. *IEEE Spectr.* 54, 3 (March 2017), 32–37. <https://doi.org/10.1109/MSPEC.2017.7864754>
- [41] Tianqi Wang, Chao-Kai Wen, Hanqing Wang, Feifei Gao, Tao Jiang, and Shi Jin. 2017. Deep learning for wireless physical layer: Opportunities and challenges. *China Communications* 14, 11 (2017), 92–111. <https://doi.org/10.1109/CC.2017.8233654>
- [42] Xiaofei Wang, Yiwen Han, Chenyang Wang, Qiyang Zhao, Xu Chen, and Min Chen. 2019. In-Edge AI: Intelligentizing Mobile Edge Computing, Caching and Communication by Federated Learning. *IEEE Network* 33, 5 (2019), 156–165. <https://doi.org/10.1109/MNET.2019.1800286>
- [43] Yu Wang, Jie Yang, Miao Liu, and Guan Gui. 2020. LightAMC: Lightweight Automatic Modulation Classification via Deep Learning and Compressive Sensing. *IEEE Transactions on Vehicular Technology* 69, 3 (2020), 3491–3495. <https://doi.org/10.1109/TVT.2020.2971001>
- [44] Nathan E. West and T. O’Shea. 2017. Deep architectures for modulation recognition. *2017 IEEE International Symposium on Dynamic Spectrum Access Networks (DySPAN)* (2017), 1–6.
- [45] Aston Zhang, Zachary C. Lipton, Mu Li, and Alexander J. Smola. 2021. Dive into Deep Learning. *arXiv preprint arXiv:2106.11342* (2021).
- [46] Maede Zolanvari, Marcio A. Teixeira, Lav Gupta, Khaled M. Khan, and Raj Jain. 2019. Machine Learning-Based Network Vulnerability Analysis of Industrial Internet of Things. *IEEE Internet of Things Journal* 6, 4 (2019), 6822–6834. <https://doi.org/10.1109/JIOT.2019.2912022>